



# The application of detrended fluctuation analysis to assess physical characteristics of the human cell line ECV304 following toxic challenges

Yasser Abd Djawad<sup>a,\*</sup>, David Attwood<sup>b</sup>, Janice Kiely<sup>b</sup>, Richard Luxton<sup>b</sup>

<sup>a</sup> Electronics Department, Universitas Negeri Makassar, Indonesia

<sup>b</sup> Institute of Biosensing Technology, University of the West of England, UK



## ARTICLE INFO

### Keywords:

Cell toxicity  
Impedance spectroscopy  
Morphological size changes

## ABSTRACT

In this paper we present a non-contact, impedance-based sensor system capable of characterizing the toxic response of cells to three different types of toxin. ECV304 cells were treated with 1 mM Hydrogen peroxide, 5% Dimethyl Sulfoxide, and 10 µg/ml saponin. Impedance spectroscopy was performed over a 2 h period on the cells within a commercial cell growth chamber, positioned on a pair of measurement electrodes, at frequencies between 200 and 830 kHz at 10 kHz intervals. Analysis of the impedance data was undertaken using the feature-extraction technique, Detrended Fluctuation Analysis (DFA). DFA scales the autocorrelation of a non-stationary signal, such as those generated using impedance spectroscopy for cytotoxicity testing. The correlation between the average fluctuation of the signal,  $F(n)$  (and scaling exponent,  $\alpha$ ) and a measurement of the cell size from image analysis was evaluated. The results showed that  $F(n)$  and  $\alpha$  were strongly related to the changes of the morphological size of the cells. The results demonstrated that non-contact impedance spectroscopy, coupled with DFA can be used to monitor cell size in real time.

## 1. Introduction

A number of biochemical tests, based on the measurement of colour, are widely used to evaluate the toxicity of a drug or chemical by assessing viability of cells challenged with a potential toxin. These traditional approaches involve a number of steps and consequently they are inappropriate for real time or continuous monitoring. A number of techniques based on electrical measurements have been developed by researchers to study and monitor cell behaviour and viability [1–4]. Impedance spectroscopy is one such method and, because it can be miniaturised and gives instantaneous data, it has the potential to be applied for the continuous monitoring of cells in culture [5–7]. Cytotoxic changes in cells have been demonstrated using impedance spectroscopy as a result of exposure to toxins and also viruses [1,5].

Classical methods for analysing data from impedance spectroscopy to study behaviour of the biological systems have been reported by many researchers. Commonly these methods used to analyse the impedance signal generated by the cells focus on either time domain or frequency domain analysis [6,8–12]. However, the analysis of the time or frequency domains alone can lead to an oversimplified understanding of the cells response to toxins. Therefore, Time-Frequency Representations (TFRs) have been applied to give a more complete representation of the data generated from monitoring toxin related

changes in cells [13]. Short Time Fourier Transform (STFT) was used to discriminate three types of cells (Jurkat, ECV304 and Caco2) [14]. This work demonstrated that each type of cell generated a unique signal and STFT was able to distinguish the characteristics of those signals. Furthermore, another TFR technique, the Discrete Wavelet Transform (DWT) has been used to extract features from Electroencephalogram (EEG) signals [13,15]. However, the challenge of these TFRs techniques is that a very large data set is generated; this then requires the application of reducing techniques in order to create a smaller, more manageable data package. Wavelet Package Decomposition was also used to characterise impedance spectroscopy signals from ECV304 cells treated with Hydrogen peroxide ( $H_2O_2$ ) [16]. The signals from the cells were characterised using the coefficients derived from the decomposition algorithm, which related to the cell morphology. The advantage of this approach is that it gave a systematic process for characterisation of the large data sets obtained from cell monitoring experiments using impedance spectroscopy giving a route to automated data analysis.

Other data processing techniques also provide alternatives to analysing large data sets obtained from biomedical experiments. One such technique is Detrended Fluctuation Analysis (DFA), which is a statistical method for scaling long-range correlations. Advantages of DFA over other methods (e.g. spectral analysis and Hurst analysis) are that it permits the detection of intrinsic self-similarity embedded in a

\* Corresponding author.

E-mail address: [yasser.djawad@unm.ac.id](mailto:yasser.djawad@unm.ac.id) (Y.A. Djawad).

<https://doi.org/10.1016/j.sbsr.2019.100269>

Received 10 November 2018; Received in revised form 21 February 2019; Accepted 27 February 2019

2214-1804/ © 2019 The Authors. Published by Elsevier B.V. This is an open access article under the CC BY-NC-ND license (<http://creativecommons.org/licenses/by-nc-nd/4.0/>).

seemingly non-stationary time series, and avoids the spurious detection of apparent self-similarity, which may be an artefact of extrinsic trends. DFA has been used to analyse biosignals generated by cells and organs, for example, to investigate the fluctuation properties of an ion channel [17] and to model patterns of breathing [18]. In another example, DFA was used in biomedical signal processing for the discrimination of heart rate variability between children with type 1 diabetes with micro-albuminuria and healthy children [19].

In this study, a cytotoxicity test was developed using ECV304 cells to investigate the response to three different toxins and impedance data was analysed using DFA. Key parameters created using the DFA method, the fluctuation average  $F(n)$  and the scaling exponent,  $\alpha$ , were correlated with cell size changes as observed via microscopy. The toxins and their concentrations were selected based on their physical properties and mechanism of toxicity. Toxins used were  $H_2O_2$ , a potent oxidising agent; Dimethyl Sulfoxide (DMSO), a potent cell differentiating agent; and saponin, a potent membrane permeabilizing agent.  $H_2O_2$  is used in the food and pharmaceutical industries and is reported to cause cell damage through direct oxidation of lipids, proteins and DNA [20,21]. The main applications for DMSO are found in the food, pharmacy and agrochemicals sectors. A previous study showed that DMSO changed the morphology of cells and, depending upon the concentration, reduced the cell viability [22]. Saponins are mostly used in the pharmaceutical and cosmetic industry. Saponin is a detergent-like molecule that is able to permeabilise the plasma membrane of the cells. Saponin penetrates the lipid bilayer structure of the cells and binds with the cholesterol to lyse cells [23].

## 2. Materials and methods

### 2.1. Cells preparation

ECV304 cells, from the European Collection of Cell Cultures (Public Health England) were seeded at a density of  $3 \times 10^5$  cells/mL in a  $75 \text{ cm}^3$  flask in 12 mL M199 media (Gibco) supplemented with 10% foetal calf serum and 2 mL L-glutamine and maintained in a humidified incubator at  $37^\circ\text{C}$  with 5%  $\text{CO}_2$ . The medium was changed every 3 days to feed the cells and monitored daily by microscope to check for confluence, at which point the cell monolayer covers 75–80% of flask surface. The 70–80% confluence was estimated by observing and comparing space occupied by the cells with the area that is not occupied by the cells. When confluence was achieved, the cell layer was washed with Phosphate Buffered Saline (PBS) followed by 1 mL of Trypsin-EDTA solution (0.05% porcine trypsin, 0.2 g/L EDTA) followed by incubation at  $37^\circ\text{C}$  for approximately 5 min to allow the cells to detach from the flask surface. Once the cells had detached, the trypsin was neutralised by the addition of 2 mL of growth medium and the cell density calculated by the Trypan Blue Exclusion method. The cell suspension was diluted to a density of  $3 \times 10^5$  cells/mL and 2 mL of cell suspension added to a chamber in a 2-chamber tissue culture plate (Nunc LAB-TEK II Chambered Coverglass, USA) and maintained at  $37^\circ\text{C}$  and 5%  $\text{CO}_2$  until cell monolayer covers 100% of flask surface. Cytotoxicity testing was performed by adding 1 mM  $H_2O_2$ , 5% DMSO and 10  $\mu\text{g}/\text{ml}$  saponin. Images were recorded using Nikon phase contrast microscope (Nikon Instruments Inc., USA) at a magnification of 200 at 1, 80 and 120 min for each toxic challenge.

### 2.2. Instrumentation

Impedance measurements were conducted using the D patterned electrodes connected to a lock-in amplifier (LIA) [24]. The electrode was produced using PCB fabrication techniques and comprised a copper layer coated with  $0.1 \mu\text{m}$  gold over  $5 \mu\text{m}$  nickel. The diameter of each sensor was 22 mm, with 1 mm space between the counter and detecting electrodes, the total sensor area corresponding to the culture area of the cell chamber. The D patterned sensor was connected in series with a

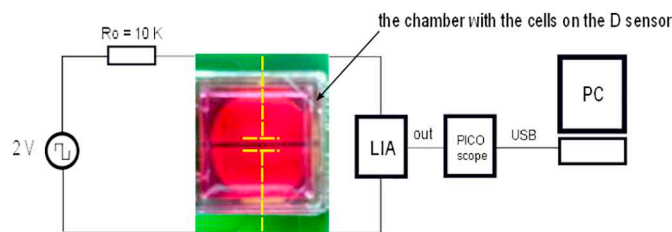


Fig. 1. Circuit diagram of the system and a photograph of the D sensors below the cell chamber.

$10 \text{ k}\Omega$  resistor to limit the current and to achieve a large bandwidth for the RC circuit. Measurements were performed by connecting the lock-in amplifier in parallel with the sensors as shown in Fig. 1. The tissue culture chamber was placed on the D sensor such that the chamber containing the cells was accurately located above the sensor, but not in direct contact with the sensor. The base of the tissue culture chamber was made of borosilicate glass with a thickness of 0.15 mm and the culture area was  $4.2 \text{ cm}^2$ . It was critical that the base of the chamber incorporated thin glass to ensure that the electric field penetrated into the cell culture. During the experiments, the D sensors with the cell chamber were placed in the incubator. The input signal, was a 2 V square wave signal over a frequency range of 200 to 830 kHz and the measurement of voltage output from the LIA was facilitated using a PICOscope. A PICOscope is a real time PC-based digital oscilloscope, which has function of digital storage oscilloscope, spectrum analyser and signal generator (Pico Technology, UK). This frequency range was selected as it had been demonstrated that significant changes in the impedance spectra occurred on the application of a toxic challenge to ECV304 cells over this frequency range [25]. Data was acquired for each data set at 1, 80 and 120 min after either  $H_2O_2$ , DMSO or saponin had been added. The total data set from each experiment comprised of 64 blocks; sampled from 200 kHz to 830 kHz with an interval 10 kHz.

### 2.3. Detrended fluctuation analysis

DFA is a statistical technique for scaling long range correlations in a time series. It quantifies the complexity of signals by first least square fitting a line to an integrated time series and subtracting that fit (the mean). Subsequently the root mean square of the fluctuations around this fit is found and this is repeated for multiple time scales, as described below.

For a 1-D time series  $X(i)$ ,  $i = 1, \dots, N$ , where  $N$  is the length of the time series. The integral of the time series can be computed using following formula:

$$y(k) = \sum_{i=1}^k (X(i) - X_{\text{avg}}) \quad (1)$$

where  $X_{\text{avg}}$  is the mean value of the time series  $X(i)$ . The integrated time series is divided into several windows with length  $n$ , the scale of the window size. In each window, a least square line is applied to obtain best approximation of data trend or linear approximation of the data. The average fluctuation  $F(n)$  of the signal in the trend can be described as:

$$F(n) = \sqrt{\frac{1}{N} \left( \sum_{k=1}^N (y(k) - y_n(k))^2 \right)} \quad (2)$$

Different values of  $n$ , the data scale, are selected and corresponding values of  $F(n)$  are calculated. To analyse the result, a plot of  $\log F(n)$  versus  $\log n$  is created and the slope of the data trend from this graph is determined as the scaling exponent,  $\alpha$ . The scaling exponent represents the autocorrelation of the time series with following criteria:

1.  $\alpha < 0.5$  anti-correlated signal.

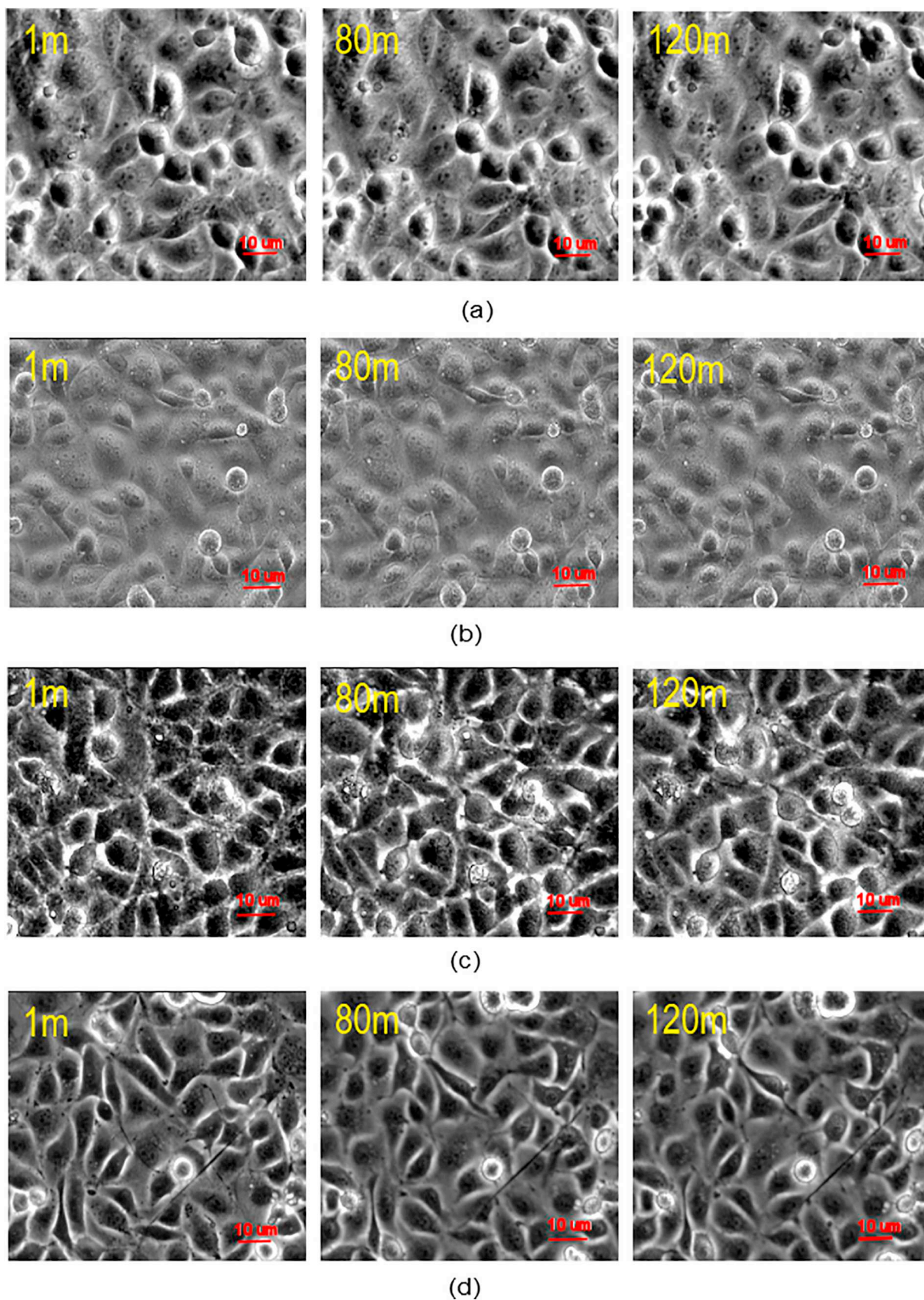


Fig. 2. Images of ECV304 cells with 3 type of toxins (a) Control cells (b) 1 mM H<sub>2</sub>O<sub>2</sub> (c) 5% DMSO (d) 10 µg/ml saponin.

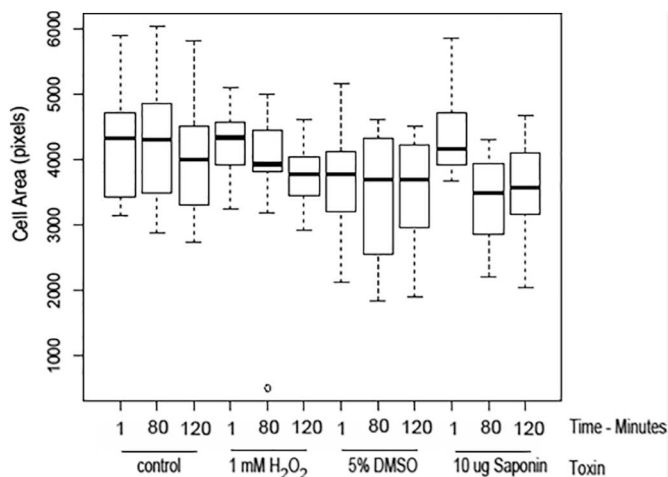


Fig. 3. Box and whiskers plot of cell size measurement using different types of toxin.

2.  $\alpha \approx 0.5$  uncorrelated signal (white noise).
3.  $\alpha >$  positive autocorrelation in the time series.
4.  $\alpha \approx 1/f$  noise.
5.  $\alpha \approx 1.5$  Brownian noise or random walk.

### 3. Results and analysis

#### 3.1. Image analysis

Images were captured and cell sizes were measured using Image-J for 10 cells in each image at 1, 80 and 120 min for each type of toxin as shown in Fig. 2. The cell size was expressed as the measured area from the image expressed by pixel number.

Fig. 3 shows Box and Whiskers plots of the cell area derived from the images. For the control cells and those treated with DMSO there was no significant change in cell size over the 180 min the measurements were made. Cells treated with  $H_2O_2$  showed a significant reduction in cell size across the three time points. For cells treated with saponin there was a significant reduction in cell size between 1 min and 80 min of exposure ( $p < 0.01$ ) whereas there was not a significant difference in the cell size between 80 and 120 min exposure to saponin. This implies that by 80 min the cells had recovered from the stress associated with the addition of saponin.

#### 3.2. Detrended fluctuation analysis

DFA was conducted on the impedance spectroscopy data obtained for control cells and those treated with  $H_2O_2$ , DMSO and saponin. The data used was the difference data obtained from subtracting the spectra of the media from that of the spectra of the media and cells, as shown in Fig. 4. The difference spectra were then segmented into 64 data batches sampled from 200 kHz to 830 kHz with an interval of 10 kHz.

Fig. 5 illustrates the average fluctuation  $F(n)$  for ECV304 cells following exposure to the three toxins, and control, for 1, 80 and 120 min for each scale, i.e. the number of segments the total data set is divided, each containing a number of 10 kHz data sets. In all cases the magnitude of the average fluctuation,  $F(n)$ , increased with the scale. This is as expected because as the scale increases the number of data sets used in the analysis increases. For example, for the control sample,  $F(n)$  is  $\approx 885$  when a scale of 6 is used and  $F(n) \approx 2795$  for a scale of 24. For all the treatments at 1 min exposure there was a mean 1.85 fold increase in  $F(n)$  going from scale 6 to scale 12 and a mean 1.75 fold increase in  $F(n)$  going from scale 12 to 24. This was consistent across all the exposure times.

The range of  $F(n)$  did vary with the treatments. For the control cells

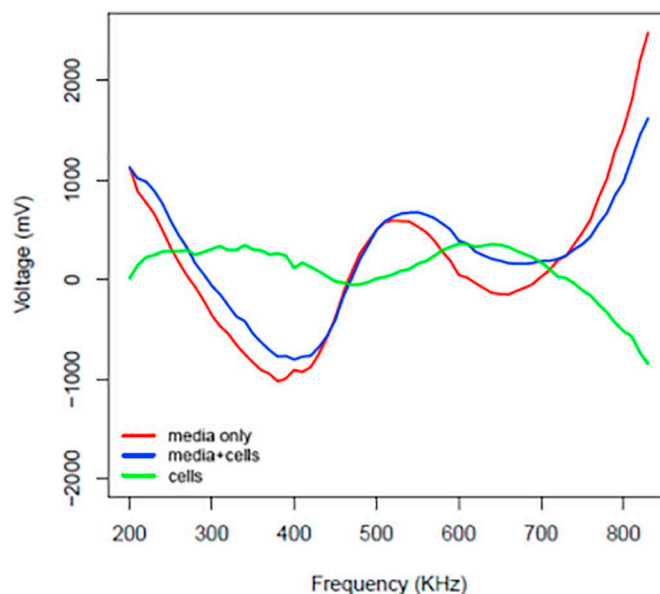


Fig. 4. IS spectra and IS difference spectra from cells and media.

the range of  $F(n)$  varied slightly across the exposure times was 5 for scale 6, 10 for scale 12 and 14 for scale 24. For cells treated with saponin, compared with the control treatment there was no significant change in the  $F(n)$  range at scales 6 and 12, but an increased range of 75 at scale 24. There was a significant difference in the  $F(n)$  range for cells exposed to  $H_2O_2$  or DMSO compared with the control, at all times with the range reaching 200 for  $H_2O_2$  treated cell and 280 for DMSO treated cells, for scale 24. This suggests that the data has higher levels of fluctuation in cells treated with toxins with DMSO.

The control cells showed that the values of  $F(n)$  on the scale 6 and the scale 12 tend to decrease at 80 min and increase at 120 min but at scale 24 there was a generalised decrease of  $F(n)$  values over all time periods as shown by Fig. 5a. When cells were exposed to  $H_2O_2$ ,  $F(n)$  decreased with exposure time. This was seen at all scales as shown in Fig. 5b. Cells treated with 5% DMSO showed the greatest  $F(n)$  values and the greatest range of values. All the scales showed similar changes over time with a decrease in  $F(n)$  between 1 and 80 min followed by an increase between 80 and 120 min as seen in Fig. 5c. Fig. 5d shows the graph of cells +  $10 \mu\text{g/ml}$  saponin and depicts different patterns for each scale used. As noted above, the  $F(n)$  values were not significantly different from those obtained from the controls except at scale 24.

Increasing  $F(n)$  values indicate increasing fluctuation in the impedance spectra obtained from the cells. The toxins used are well known to cause cell disruption which can result in changes of cell size and alteration of the internal structure of the cells, both of which can affect the impedance of the cell. The results suggest that for cells treated with  $H_2O_2$  or saponin there is a significant decrease in cell size which results in a reduction in the fluctuation of in the impedance signal. Treatment with DMSO resulted in the highest values of  $F(n)$  observed indicating the greatest level of fluctuation in the impedance signal derived from the cells. The  $F(24)$  values did not show a linear trend as did the other toxins which may reflect the lack of change in cell size over time. The higher values of  $F(n)$  may be a result of the greater variability in the cell size as indicated by the interquartile distance in Fig. 3. Although there was not a significant change in cell size the results suggest that 5% DMSO significantly disrupts cells by affecting the internal structure of the cells whilst not changing of cell size over time.

At scale 24 there is a correlation between the  $F(n)$  and cell size for cells treated with hydrogen peroxide and saponin, as shown in Fig. 3. In both cases the change in cell size over time is reflected in the change of  $F(n)$  over time. At scale 24 the control cells demonstrated a drop in  $F(n)$  over time but the magnitude of the drop was only 14. Although there

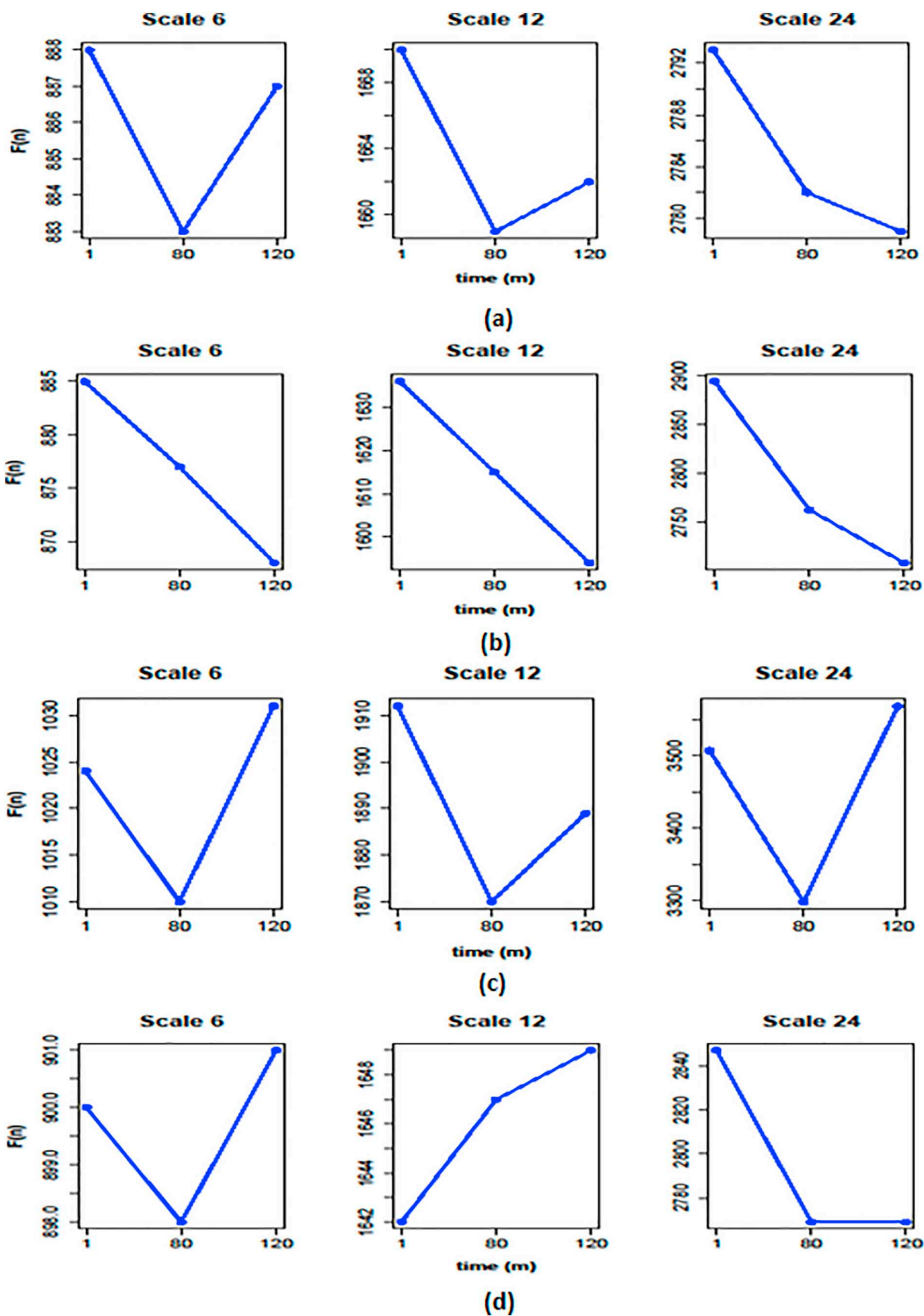


Fig. 5. The average fluctuation F(n) of (a) Control cells (b) cells + H<sub>2</sub>O<sub>2</sub> (c) cells + DMSO (d) cells + saponin.

**Table 1**

Correlation coefficients between cell size and the average fluctuation of the signals and F(n) value calculated using DFA.

Treatments	F(n)		
	6	12	24
Control	0.1890	0.7034	0.9496
1 mM H <sub>2</sub> O <sub>2</sub>	0.9508	0.9607	0.9989
5% DMSO	0.6546	0.9989	0.7374
10 µg/ml saponin	0.4193	0.8660	0.9707

**Table 2**

Scaling exponent ( $\alpha$ ) of the four treatments of the ECV304 cells.

Treatments	1 m	80 m	120 m
Control	0.8326	0.8185	0.8181
1 mM H <sub>2</sub> O <sub>2</sub>	0.8597	0.8362	0.8296
5% DMSO	0.8897	0.8596	0.8914
10 µg/ml saponin	0.8361	0.8226	0.8203

was not a statistical difference in cell size over time there is a strong correlation between F(n) at scale 24 and the median cell size. Cells exposed to 5% DMSO demonstrated a drop in F(n) from 1 min to 80 min and then an increase in F(n) from 80 min to 120 min which is not reflected in the change in cell size. It is noted that the interquartile range increased significantly at 80 min compared with the range at 1 min. The interquartile range then decreased at 120 min. Correlation coefficients between cells size measured from microscopy images and F(n) are shown in Table 1. These clearly show the strong correlation between the mean cell size and the F(n) at scale 24. Cells exposed to DMSO show the greatest correlation at scale 12. These results imply that F(n) correlates well with cell size and reflects changes in cell size for certain toxins, in particular a highly significant correlation was observed for the effect of H<sub>2</sub>O<sub>2</sub> on cell size over time.

In addition to measuring F(n), the scaling exponent ( $\alpha$ ) was calculated for the control and three treatments of ECV304 cells. The values of  $\alpha$  at 1, 80 and 120 min are presented in Table 2. Firstly, all values were greater than 0.8, which in accordance with DFA theory suggests that the noise associated with the signal was not increasing as a function of the scale used. The pattern of change of values over time were markedly similar to the patterns of change seen with F(n) at the scale of 24 over the three time periods. This may indicate that a scale of 24 provides a more accurate result in comparison with the scales 6 or 12 and it is noted that the impedance data at the different time points showed positive autocorrelation, as all the scaling exponents,  $\alpha$ , of the time series were above 0.8.

A strong correlation between cell size and the scaling exponent,  $\alpha$ , was found for all the treatments: Control = 0.8778, H<sub>2</sub>O<sub>2</sub> = 0.994, DMSO = 0.8412, saponin = 0.9295. This is as expected as there is the strong similarity between the change in  $\alpha$  and F(24). Apart from the treatment with DMSO the correlation coefficients of time versus scaling exponent were lower than the corresponding correlation coefficients of time versus F(24).

#### 4. Conclusions

In this study, ECV304 cells were challenged with three toxins to induce cytotoxic changes in the cells. The toxins used have different mechanisms of toxicity resulting in cell changes which result in changes in the cell size with or without changes to the internal organelles of the cells. Images of the cells were taken over 120 min and changes in size noted. Impedance spectra of the cells were collected at 1 min, 80 min and 120 min of exposure to the toxins. The application of DFA on the impedance spectra was investigated as a method that could rapidly detect cell toxicity.

The results of DFA were compared with the measurement of cell size resulting from the toxic-challenge. A strong positive correlation was observed with F(24). In addition, the scaling exponents ( $\alpha$ ) also provided strong positive correlation with the cell size measurements. Cells treated with 1 mM H<sub>2</sub>O<sub>2</sub> demonstrated the strongest correlation between changes measured by microscopy and changes measured by impedance data. Cells treated with 5% DMSO did not show a significant change in size and F(n) did not show a linear trend with time at all scales. The very high values compared with the control cell suggest that the cytotoxic effects of DMSO involve changes to the cell organelles.

The work reported suggests that an automated measure of the health of cells could be developed using impedance spectroscopy coupled with signal analysis using the DFA technique. Monitoring of the magnitude and the change in F(n) over time could indicate different cytotoxic effects on the cells in terms of cell size or changes in cell organelles. More work using a wider range of toxins could lead to the development of an algorithm that could accurately determine the effect of a toxin on the cell and aid the classification of cytotoxic effects of different chemicals.

#### Conflict of interest

None.

#### References

- [1] C. Caviglia, K. Zr, S. Canepa, M. Carminati, L.B. Larsen, R. Raiteri, T.L. Andresen, A. Heiskanen, J. Emnus, Interdependence of initial cell density, drug concentration and exposure time revealed by real-time impedance spectroscopic cytotoxicity assay, *Analyst* 140 (10) (2015) 3623–3629, <https://doi.org/10.1039/C5AN00097A> URL <https://pubs.rsc.org/en/content/articlelanding/2015/an/c5an00097a>.
- [2] R.Y.A. Hassan, M.M. Mekawy, P. Ramnani, A. Mulchandani, Monitoring of microbial cell viability using nanostructured electrodes modified with graphene/alumina nanocomposite, *Biosens. Bioelectron.* 91 (2017) 857–862, <https://doi.org/10.1016/j.bios.2017.01.060> URL <http://www.sciencedirect.com/science/article/pii/S0956566317300593>.
- [3] O. Salyk, J. Vteek, L. Omasta, E. afakov, S. Stesek, M. Vala, M. Weiter, Organic electrochemical transistor microplate for real-time cell culture monitoring, *Appl. Sci.* 7 (10) (2017) 998, <https://doi.org/10.3390/app7100998> URL <http://www.mdpi.com/2076-3417/7/10/998>.
- [4] N. Gaio, A. Waafi, M.L.H. Vlaming, E. Boschman, P. Dijkstra, P. Nacken, S.R. Braam, C. Boucsein, P.M. Sarro, R. Dekker, A multiwell plate organ-on-chip (OOC) device for in-vitro cell culture stimulation and monitoring, *IEEE Micro Electro Mech. Syst. (MEMS)* 2018 (2018) 314–317, <https://doi.org/10.1109/MEMSYS.2018.8346549>.
- [5] M.S. Cheng, S.H. Lau, K.P. Chan, C.-S. Toh, V.T. Chow, Impedimetric cell-based biosensor for real-time monitoring of cytopathic effects induced by dengue viruses, *Biosens. Bioelectron.* 70 (2015) 74–80, <https://doi.org/10.1016/j.bios.2015.03.018>.
- [6] E. Sarr, M. Lecina, A. Fontova, F. Gdia, R. Brags, J.J. Cair, Real-time and on-line monitoring of morphological cell parameters using electrical impedance spectroscopy measurements, *J. Chem. Technol. Biotechnol.* 91 (6) (2016) 1755–1762, <https://doi.org/10.1002/jctb.4765> URL <https://onlinelibrary.wiley.com/doi/abs/10.1002/jctb.4765>.
- [7] D. Seidel, J. Obendorf, B. Englich, H.-G. Jahnke, V. Semkova, S. Haupt, M. Girard, M. Peschanski, O. Brstle, A.A. Robitzki, Impedimetric real-time monitoring of neural pluripotent stem cell differentiation process on microelectrode arrays, *Biosens. Bioelectron.* 86 (2016) 277–286, <https://doi.org/10.1016/j.bios.2016.06.056>.
- [8] C. Dalmay, M. Cheray, A. Pothier, F. Lallou, M.O. Jauberteau, P. Blondy, Ultra sensitive biosensor based on impedance spectroscopy at microwave frequencies for cell scale analysis, *Sensors Actuators A Phys.* 162 (2) (2010) 189–197, <https://doi.org/10.1016/j.sna.2010.04.023> URL <http://www.sciencedirect.com/science/article/pii/S0924424710001998>.
- [9] L. Wang, L. Wang, H. Yin, W. Xing, Z. Yu, M. Guo, J. Cheng, Real-time, label-free monitoring of the cell cycle with a cellular impedance sensing chip, *Biosens. Bioelectron.* 25 (5) (2010) 990–995, <https://doi.org/10.1016/j.bios.2009.09.012>.
- [10] M.A. Ahmad, Z.A. Natour, S. Attoub, A.H. Hassan, Monitoring of the budding yeast cell cycle using electrical parameters, *IEEE Access* 6 (2018) 19231–19237, <https://doi.org/10.1109/ACCESS.2018.2820080>.
- [11] C. Slouka, D. J. Wurm, G. Brunauer, A. Welzl-Wachter, O. Spadiut, J. Fleig, C. Herwig, A novel application for low frequency electrochemical impedance spectroscopy as an online process monitoring tool for viable cell concentrations, *Sensors (Basel, Switzerland)* 16 (11). doi:<https://doi.org/10.3390/s16111900>. URL <https://www.ncbi.nlm.nih.gov/pmc/articles/PMC5134559/>
- [12] J.B.J.H. van Duuren, M. Musken, B. Karge, J. Tomasch, C. Wittmann, S. Hussler, M. Brnstrup, Use of single-frequency impedance spectroscopy to characterize the growth dynamics of biofilm formation in *Pseudomonas aeruginosa*, *Sci. Rep.* 7 (1) (2017) 5223, <https://doi.org/10.1038/s41598-017-05273-5> URL <https://www>.

- [nature.com/articles/s41598-017-05273-5](https://doi.org/10.1016/j.cellbi.2007.09.001).
- [13] S.E. Khaleelulla, P.R. Kumar, EEG signal analysis for mental states and conditions of human brain, Proceedings of 2nd International Conference on Micro-Electronics, Electromagnetics and Telecommunications, Lecture Notes in Electrical Engineering, Springer, Singapore, 2018, pp. 141–151, [https://doi.org/10.1007/978-981-10-4280-5\\_15](https://doi.org/10.1007/978-981-10-4280-5_15).
- [14] Z. Wang, J. Kiely, M. Nibouche, R.W. Luxton, Z. Wang, J. Kiely, M. Nibouche, R.W. Luxton, Impedimetric discrimination of cell types for use in a whole cell biosensor, Proceedings of the 10th World Congress on Biosensors, Elsevier, Shanghai, China, 2008 URL <http://www.sparkdesigns.co.uk/workingfiles/bluezulu/biosensors08/index.htm>.
- [15] V. Geethu, S. Santhoshkumar, An efficient FPGA realization of seizure detection from EEG signal using wavelet transform and statistical features, IETE J. Res. (2018) 1–11, <https://doi.org/10.1080/03772063.2018.1491806>.
- [16] Y.A. Djawad, J. Kiely, M. Nibouche, P. Wraith, R. Luxton, Robust feature extraction from impedimetric signals using wavelet packet decomposition with application to cytotoxicity testing, IET Sci. Meas. Technol 6 (6) (2012) 456–463, <https://doi.org/10.1049/iet-smt.2012.0009>.
- [17] T.-H. Lan, Z.-Y. Gao, A.N. Abdalla, B. Cheng, S. Wang, Detrended fluctuation analysis as a statistical method to study ion single channel signal, Cell Biol. Int. 32 (2) (2008) 247–252, <https://doi.org/10.1016/j.cellbi.2007.09.001> URL <http://www.sciencedirect.com/science/article/pii/S1065699507002338>.
- [18] B.F. BuSha, G. Banis, A stochastic and integrative model of breathing, Respir. Physiol. Neurobiol. 237 (2017) 51–56, <https://doi.org/10.1016/j.resp.2016.12.012>.
- [19] A. Golińska, Detrended fluctuation analysis (DFA) in biomedical signal processing: selected examples, studies in logic, Grammar Rhetoric 29 (2012) 107–115.
- [20] N. Nakayama, S. Yamaguchi, Y. Sasaki, T. Chikuma, Hydrogen peroxide-induced oxidative stress activates proteasomal trypsin-like activity in human U373 glioma cells, J. Mol. Neurosci. 58 (2) (2016) 297–305, <https://doi.org/10.1007/s12031-015-0680-9>.
- [21] L. Zhou, Y. Peng, Q. Wang, Q. Lin, An ESIPT-based two-photon fluorescent probe detection of hydrogen peroxide in live cells and tissues, J. Photochem. Photobiol. B 167 (2017) 264–268, <https://doi.org/10.1016/j.jphotobiol.2017.01.011>.
- [22] R. Pal, M.K. Mamidi, A.K. Das, R. Bhonde, Diverse effects of dimethyl sulfoxide (DMSO) on the differentiation potential of human embryonic stem cells, Arch. Toxicol. 86 (4) (2012) 651–661, <https://doi.org/10.1007/s00204-011-0782-2>.
- [23] R. Malabed, S. Hanashima, M. Murata, K. Sakurai, Sterol-recognition ability and membrane-disrupting activity of Ornithogalum saponin OSW-1 and usual 3-O-glycosyl saponins, Biochim. Biophys. Acta 1859 (12) (2017) 2516–2525, <https://doi.org/10.1016/j.bbamem.2017.09.019>.
- [24] S.K. Sengupta, J.M. Farnham, J.E. Whitten, A simple low-cost lock-in amplifier for the laboratory, J. Chem. Educ. 82 (9) (2005) 1399, <https://doi.org/10.1021/ed082p1399>.
- [25] Y.A. Djawad, J. Kiely, P. Wraith, R. Luxton, Lock-in amplifier as a sensitive instrument for biomedical measurement: analysis and implementation, Indones. J. Electr. Eng. Comput. Sci 12 (10) (2014) 7214–7222, <https://doi.org/10.11591/ijeecs.v12.i10.pp7214-7222>.